Branched nanocrystals

DOI: 10.1002/smll.200700787

Dopant-Induced Formation of Branched CdS Nanocrystals**

Yung-Jung Hsu and Shih-Yuan Lu**

The dimensions and structures of semiconductor nanocrystals (NCs) play an important role in determining the electronic and optical properties of the materials. In the past few years, much effort has been expended to control the size and shape of these materials. One way to control NC structures is to enhance anisotropic growth using an external catalytic medium such as the metallic nanoparticles employed in vapor–liquid–solid (VLS)[1] and solution–liquid–solid (SLS)[2] processes. Another common approach using surfactants as capping agents or soft templates can be utilized in a solution system to facilitate anisotropic crystal growth.[3] Tetrapods, a unique example of these anisotropically shaped NCs, find potential applications in nanocomposites and nanoscale devices. For example, because of the three-dimensionally extending structures, tetrapods may be a promising building unit for the preparation of interesting superstructures for nanoelectronics, especially three-dimensional (3D) prototypes.[4] In addition, semiconductor tetrapods have potential advantages in hybrid NC/polymer photovoltaic devices because their 3D structures make it facile for them to orderly align toward the electrodes within the polymer film, providing a direct charge-carrier transportation pathway to improve the device performance.[5] Up to now, nanometer-sized tetrapod crystals have been synthesized for a variety of II–VI semiconductors including ZnO,[6] CdS,[7] CdSe,[8] and CdTe.[5a,9] The most often observed crystallographic feature of these tetrapod NCs is one cubic zinc blende (ZB) core attached with four hexagonal wurtzite (WZ) arms. Evidently, to form such novel architecture, one should have the crystals nucleate in the ZB phase followed by anisotropic growth in the WZ phase. The former stage can be achieved through kinetic control of the reaction and the latter can be realized with the assistance of proper capping ligands. The ability of crystals to switch from one growth mode to another during a continuous reaction is thus crucial to achieving the tetrapod growth. This, however, depends on the intrinsic property of the materials, for example, the most thermodynamically favorable crystallographic structure under specific reaction conditions. As compared to CdSe and CdTe, CdS tetrapods are much more rarely obtained in synthetic systems due to the small growth-energy difference between their WZ and ZB phases.[10] This inherent restriction makes it impractical to controllably enable clear-cut growth-phase switching and thus difficult to obtain tetrapod products without external aids. In this Communication, we report a novel approach to facilitate the formation of tetrapod-dominated branched CdS NCs by simply incorporating a trace amount of dopant in a solvothermal process. The crystallographic structure of the branched NCs is examined with high-resolution transmission electron microscopy (HRTEM), which shows that the branched structures have a ZB core and multiple WZ arms. A plausible mechanism for the growth of branched NCs is proposed and discussed.

The structures and dimensions of the as-prepared products were first investigated with scanning electron microscopy (SEM). Figure 1a shows the SEM image of CdS nanowires (NWs) obtained under the typical solvothermal reaction with $Cd(NO_3)_2$ and S powder as the reactants and ethylenediamine (EN) as the solvent. The growth of CdS NWs was guided by the capping effect of the EN present in the system. With extra feeding of a trace amount of Se powder in the reactants while keeping all other reaction parameters fixed, branched structures became the dominant product instead of NWs, as can be seen in Figure 1b. These branched structures remained dominant with high morphological yield when Te powder was fed along with the S powder as the dopant. The low-magnitude SEM images shown in Figure S1 (Supporting Information) further illustrate the high morphological yield of the tetrapod-dominated branched structures in the products. The average diameters of the NWs and branched arms were about 30 nm. The arm length of these branched structures varied from 100 to 700 nm. The atomic compositions of Se and Te in the branched NC products were around 5% and 2.5%, respectively, as determined from the TEM-EDS (TEM-energy dispersive spectrometry) analyses. The crystallographic structures of the as-synthesized samples were further characterized with X-ray diffraction (XRD) and HRTEM.

Figure S2 shows the XRD patterns of the three CdS-based nanostructures. All three samples predominantly show the diffraction behavior of WZ CdS. A slight variation in the positions of diffraction peaks was observed among the three samples from a careful examination of the more focused XRD spectra shown in Figure 1d. For CdS NWs, the diffraction peak at a 2θ value of 26.5° corresponds well to the WZ(0002) planes with a d spacing of 0.336 nm, as determined from Bragg's law. For the Se-doped and Te-doped samples, the 2θ value of around 26.3° gives an interplanar spacing of 0.339 nm for the WZ(0002) planes. The slight expansion of the lattice in doped samples was due to the partial replacement of S with Se or Te atoms, which are of larger atomic size. The detailed crystal structures of the as-synthesized samples were

[*] Prof. Y.-J. Hsu
Department of Materials Science and Engineering
National Chiao Tung University
Hsinchu, Taiwan 30010 (Republic of China)
Fax: (+886) 3 5724727
E-mail: yhsu@cc.nctu.edu.tw
Prof. S.-Y. Lu
Department of Chemical Engineering
National Tsing-Hua University
Hsinchu, TAIWAN 30043 (Republic of China)
Fax: (+886) 3 5715408
E-mail: sylu@mx.nthu.edu.tw

[**] This work was financially supported by the National Science Council of the Republic of China (Taiwan) under grant NSC-96-2218-E-009-007 (Y.-J. Hsu) and NSC-95-2221-E-007-194 (S.-Y. Lu).

Supporting Information is available on the WWW under http://www.small-journal.com or from the author.

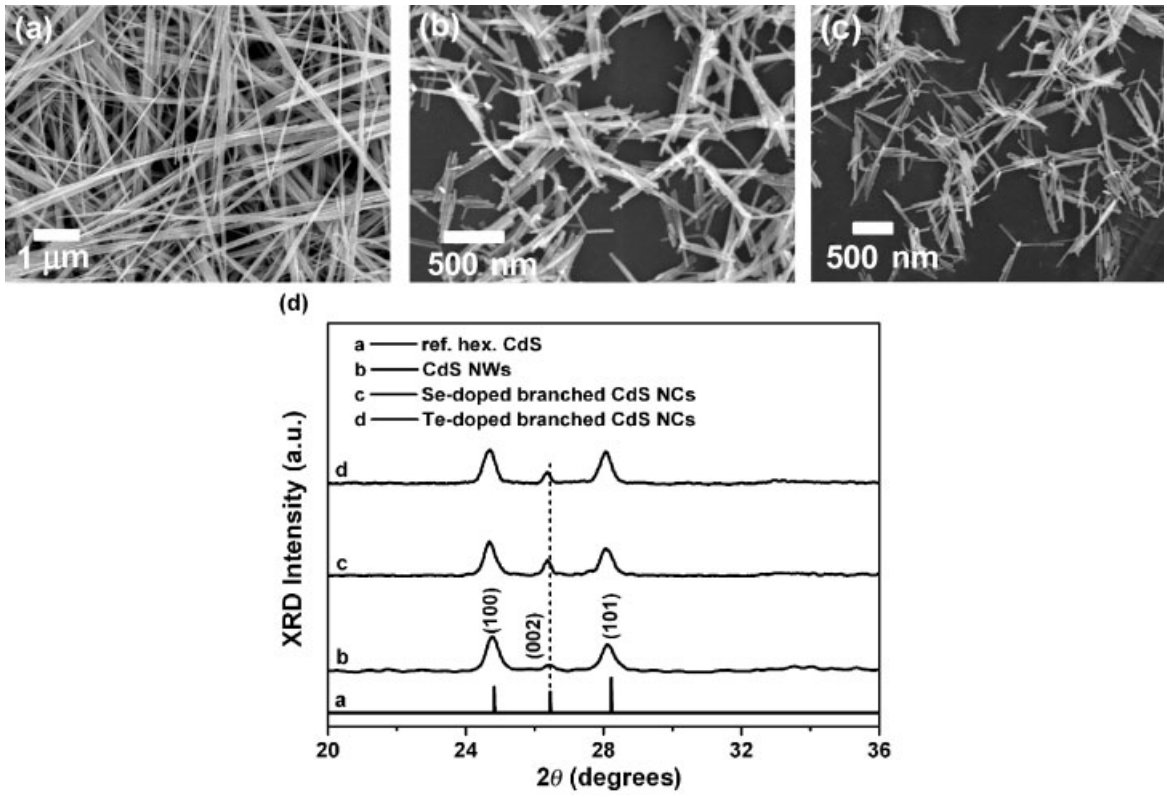

Figure 1. SEM images of a) CdS NWs, b) Se-doped CdS, and c) Te-doped branched CdS NCs. d) XRD patterns of the as-synthesized samples with the reference hexagonal CdS (JCPDS#06-0314) included for comparison.

analyzed with HRTEM. Figure 2 shows the HRTEM images of an individual NW, Se-doped tripod, and Te-doped tetrapod of CdS. Interplanar spacings of 0.67, 0.68, and 0.68 nm were observed in the axial directions of the NW and the extending arms of the Se-doped and Te-doped samples, respectively. The lattice spacings were in good agreement with the *d* spacings of the WZ (0001) planes, as determined from the corresponding XRD analyses. The axis of the NW is parallel to the WZ [0001] direction, indicating that the NWs were grown along the *c* axis. Furthermore, the arms of the Se-doped or Te-doped NCs also possessed a preferential crystalline direction along the WZ[0001] direction.

The optical properties of the three CdS-based nanostructures were characterized with UV/Vis and photoluminescence (PL) spectroscopy. As shown in Figure 3a, all three samples show an absorption edge at around 500 nm, consistent with the bulk bandgap energy of CdS ($E_g = 2.5$ eV).[11] Their corresponding PL spectra showed excitonic band-to-band emission bands centered at 508, 535, and 517 nm for the plain CdS NWs, Se-doped, and Te-doped branched CdS NCs, respectively. Their corresponding PL quantum yields (Q_s) were also evaluated and are shown in the inset of Figure 3b. As compared to the dopant-free NW samples, the significant red-shifts in emission bands of the doped branched NCs was due to the incorporation of Se and Te atoms and thus the slight reduction of bandgap energy observed in the doped samples. This result was in good agreement with those of the corresponding $CdS_{1-x}Se_x$ and $CdS_{1-x}Te_x$ films.[12]

The most common structural feature of an artificially synthesized tetrapod is a ZB core possessing four {111} facets, each attached with a WZ arm growing along the [0001] direction. In other words, tetrapods are formed when nanocrystals nucleate in the ZB phase first, followed by growth of WZ arms from the four equivalent ZB (111) facets of the tetrahedral ZB core. For the present work, we show that the same growth mechanism applies for the formation of the present Se-doped or Te-doped branched CdS NCs. To give a solid proof of the claim, we examined the phase of the cores at the core-formation stage. By suitably controlling the experimental conditions, the solvothermal reaction can be terminated at the early stage of the NC growth. The TEM images shown in Figure 4a and b give a clear illustration on the following points. For reactions with only S powder as the chalcogen source, CdS nucleated in its most stable WZ phase and grew into short nanorods along a preferential crystalline planes of (0001), which possess the smallest surface energy among all growing planes.[13] However, with the incorporation of Se or Te in the reaction, NCs of CdS tended to nucleate in the ZB phase to form nanoparticles instead of nanorods. The ZB phase of these nanoparticles can be identified from the spacing of lattice fringes and the electron-diffraction pattern shown in the two insets of Figure 4b. The existence of the ZB phase in the resulting branched NCs can be further confirmed by the HRTEM image shown in Figure 4c, taken on the intersectional region of a tripod. An evident difference in lattice fringes between the core region and the three arms was revealed, indicating distinct crystal phases therein. The lattice fringes of the three {111} facets imply that the ZB core can be attached with four arms leading to a tetrahedral structure. The three arms show a 0.34-nm interlayer spacing, which can

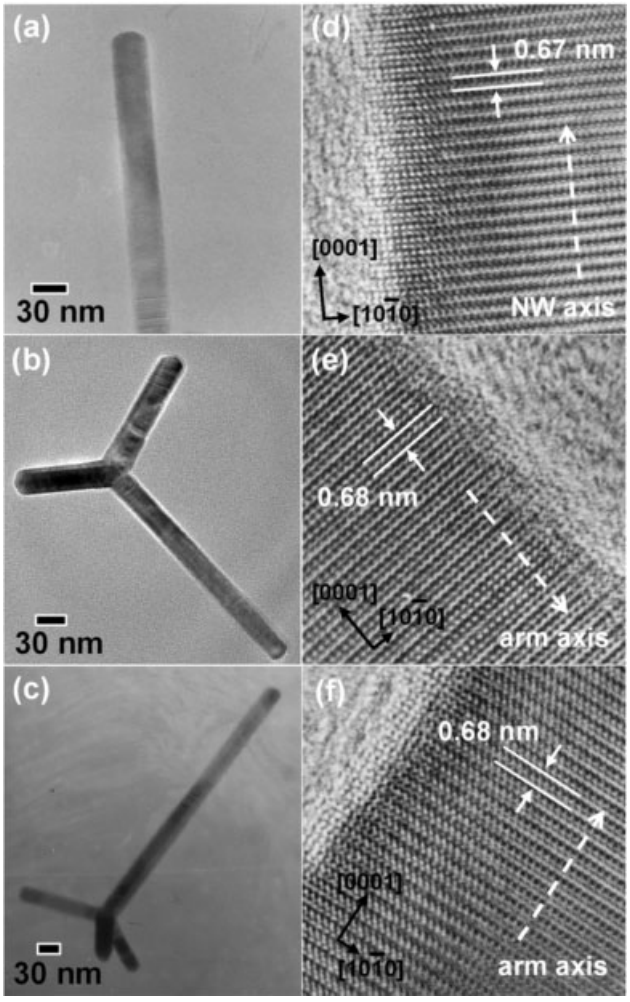

Figure 2. Typical TEM images of an individual a) CdS NW, b) Se-doped CdS tripod, and c) Te-doped CdS tetrapod. Their corresponding lattice-resolved images are shown in (d–f), respectively.

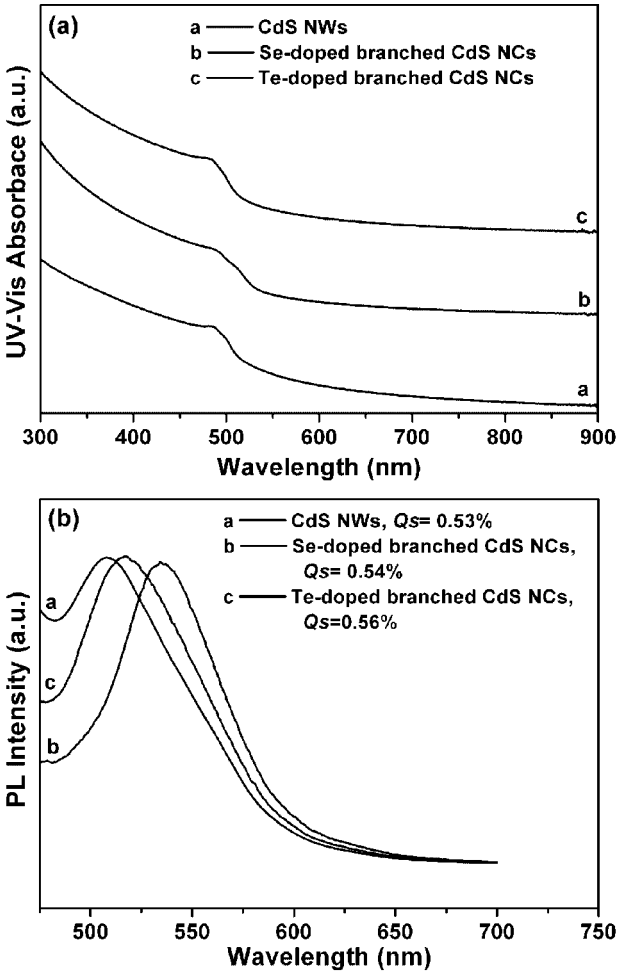

Figure 3. a) UV/Vis absorption and b) PL emission spectra for NWs, Se-doped, and Te-doped branched NCs of CdS. The excitation wavelength for PL measurement was 400 nm.

be indexed as the spacing in the WZ[0001] direction. The lattice-matched planes between the ZB core and the WZ arms imply an epitaxial relationship. From the results presented above, it can be concluded that the Se-doped and Te-doped branched CdS NCs, including tripods and tetrapods, obtained in this work possessed a ZB core with WZ arms grown out of the equivalent {111} facets of the ZB core.

Quite a few approaches for the preparation of nanometer-sized semiconductor tetrapods have been developed. Most of them are based on the growth-energy difference between the ZB and WZ phases, through which the NC growth can switch from one phase to another. Typically, through suitably controlling the temperature of growth,[7a,7b,7d,8b] the concentration of precursors,[7a,7d,8a,8b,9d] or by applying specific capping ligands in the reaction,[7c,8e,9a–9c] tetrapod NCs can be obtained in single-step processes. A two-step sequential growth technique, in which the first-prepared ZB core serve as the seeds for the subsequent growth of WZ arms, can also generate this architecture.[7b,8c,8d] For the CdTe case, the energy difference between the ZB and WZ phases is appropriately large[10] to enable easy control over the growth of the ZB core and WZ arms to form tetrapod NCs. However, it has been pointed out that this energy difference is too small to facilitate controllable tetrapod formation for CdS, CdSe, and ZnS.[5a] In our experiments, we found that it was the incorporation of dopant Se or Te that caused the formation of CdS tripods and tetrapods by increasing the energy difference between the two phases. Note that the energy difference for II–VI semiconductors between WZ and ZB phases increases monotonically as the anions become larger in atomic size.[10] It is thus reasonable that upon incorporation of Se or Te atoms, the growth-energy difference between the ZB and WZ phases for CdS is significantly enlarged. As a result, the growth of starting ZB seeds and subsequent WZ arms can proceed in a single-pot process.

To further support our arguments, we conducted the synthesis of Se-doped CdS NCs at a relatively dilute Se concentration (about 1%). As shown in Figure S3, the product was composed of a large quantity of agglomerated NWs together with a minor amount of multiarmed NCs. This outcome provided solid proof for the proposal that dopants and their concentrations play an important role in the formation of tetrapod-shaped NCs. When the dopant is present in a very limited amount (1% for the Se-doped case), the solvothermal reaction is perturbed only slightly to form

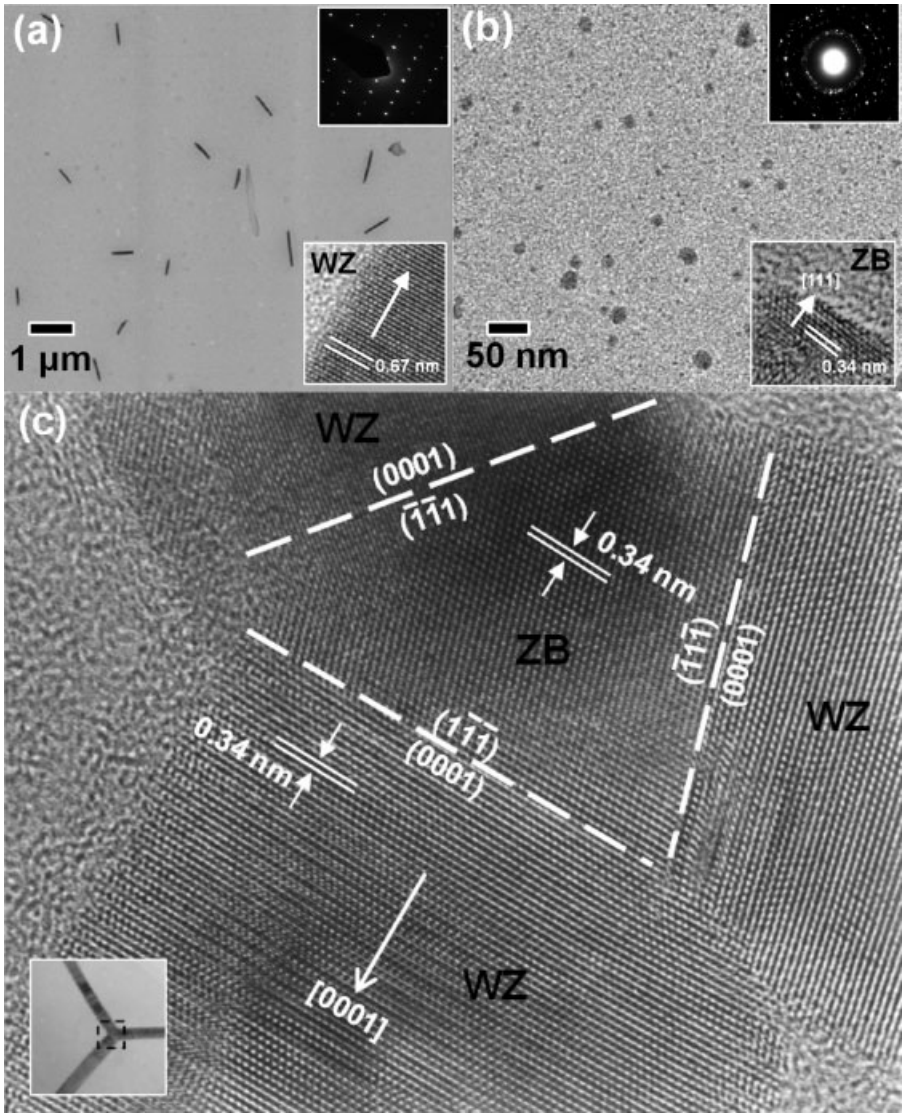

Figure 4. TEM images of a) WZ CdS and b) ZB Te-doped CdS NCs obtained at the early stage of the solvothermal process. The insets show their corresponding selected-area electron diffraction (SAED) and HRTEM images. c) HRTEM image taken on the intersectional region (as marked in the inset) of a Te-doped CdS tripod. The interfaces between the ZB core and the WZ arms are highlighted with the dashed lines.

branched NCs of limited number. At dilute dopant concentrations, the increase in energy difference between the ZB and WZ phases of CdS is quite limited, leading to only a slight change in the growth kinetics of the NCs. The presence of a relatively high concentration of dopants, however, would reverse the growth habit of CdS, making it nucleate at the ZB phase and grow at the WZ phase because of the sufficiently large energy difference between the two phases. Consequently, tripod- and tetrapod-shaped NCs in high morphological yield were obtained.

A plausible growth mechanism for the formation of Se-doped and Te-doped branched CdS NCs is proposed as follows. At the beginning of the reaction, Se and Te incorporation resulted in the growth of CdS nuclei in the ZB phase with four equivalent {111} facets exposed, as evident from the HRTEM image shown in Figure 4b. The first formed ZB CdS nanoparticles then served as the seeds from which the WZ arms grow. The arm diameter of the resulting tetrapods may be adjusted by controlling the size of the ZB seeds. Note that the lattice arrangement of Cd and S atoms on the {111} planes of ZB phase are identical to those on the WZ(0001) plane.[8a] Furthermore, the {111} planes in ZB CdS are epitaxially matched with the WZ(0002) planes due to the closeness in their d spacings ($d_{ZB}(111) \fallingdotseq d_{WZ}(0002) = 0.34$ nm). Both the atomic arrangement and lattice-spacing matches contributed to the branched CdS NC formation of this work. The solvent EN also played an important role here. In a typical case, WZ CdS NWs grew with a preferential direction along the c axis under the inducement of EN.[14] In this situation, EN tended to attach to the $\{10\bar{1}0\}$ planes and suppress the growth rate of these planes, while the (0001) planes, covered with the least amount of EN, grew the fastest. Thus, it was the different adsorption ability of EN toward different planes of CdS NCs that made the 1D growth of WZ arms possible. By suitably controlling the synthetic conditions, such as reaction temperature, heating rate, and reactant concentration, it is possible to reduce the arm diameter of the branched NCs. This task can be achieved through effective modulation of the size of the ZB seeds grown at the early stage of the solvothermal process as well as through manipulation of the relevant growth kinetics of CdS, as proposed by Manna et al.[5a] In an ideal situation, totally identical arms should be obtained in the resulting branched NCs. However, because of the inevitable local concentration fluctuations existing in the reacting system, nonequilateral arm growth may take place and even worse the growth of one or even more arms may be completely suppressed, leading to the possible appearance of three- and two-armed structures. As a final note, the Ostwald ripening effect, in which longer arms grow even longer at the expense of shorter ones, also contributed to the unequal arm lengths observed in Figure 2b and c.

In conclusion, branched CdS NCs, including tripods and tetrapods, in high morphological yield can be obtained with a simple solvothermal process by simply incorporating Se or Te as dopant into the process. It is proposed for the first time that dopant Se or Te can kinetically transform the growth habit of CdS nuclei from the typical WZ to ZB phase, thus making the formation of multiarmed structures much easier. The doping

inducement effect on the tetra- and tripod formation may give new insight into the manipulation and controllability of anisotropic nanocrystal growth. The present finding can be readily extended to other semiconductors possessing ZB–WZ polymorphism.[10]

Experimental Section

NW and branched NC syntheses: All chemicals were of analytic grade and used without further purification. The syntheses of NWs, Se-doped, and Te-doped branched NCs of CdS were carried out in a solvothermal process. For the preparation of CdS NWs, $Cd(NO_3)_2 \cdot 4H_2O$ (1.85 g, 0.006 moles) and S powder (0.19 g, 0.006 moles) were added to EN (100 mL). *Special attention should be paid when dealing with the hazardous Cd source*. After a 5 min stirring, the solution turned straw-yellow and the solution was transferred to a teflon-lined stainless steel autoclave (with a capacity of 120 mL). The autoclave was sealed, heated, and maintained at 180 °C for 24 h. For the synthesis of Se-doped branched CdS NCs, $Cd(NO_3)_2 \cdot 4H_2O$ (1.85 g, 0.006 moles), S powder (0.32 g, 0.01 moles), and Se powder (0.079 g, 0.001 moles) were used as the precursors, followed by the same procedure performed in the synthesis of CdS NWs. As to the fabrication of Te-doped branched NCs, $Cd(NO_3)_2 \cdot 4H_2O$ (1.85 g, 0.006 moles), S powder (0.32 g, 0.01 moles) and Te powder (0.128 g, 0.001 moles) were used, followed by the same reaction procedure as mentioned above. The resulting yellow solid product was centrifuged and washed with distilled water and ethanol to remove remaining ions and impurities. The product was then dried at 100 °C in vacuum for later characterization.

Characterization: The morphology and dimensions of the products were examined with field-emission scanning electron microscopy (FESEM, Hitachi S-4700). The crystallographic structure of the samples was investigated with XRD (MAC Science MXP18) and HRTEM (JEOL JEM-3000) operated at 300 kV. The compositional information was obtained with an energy dispersive spectrometer (EDS), an accessory of the HRTEM (JEM-3000). UV/Vis absorption spectra were obtained with a Hitachi U-3300 spectrophotometer. For PL spectroscopy, a Hitachi F-4500 equipped with a xenon lamp (150 W) was used. The excitation wavelength was set at 400 nm. PL quantum yield of the samples (Q_s) was determined by using tryptophan solution ($Q_{ref} = 0.16$ at a concentration of 0.73 $\mu g\ mL^{-1}$ in H_2O) as the reference. All of the absorption and emission spectra were obtained at 25 °C under ambient atmosphere.

Keywords:
cadmium sulfide · crystal growth · doping · nanostructures · tetrapods

[1] a) R. S. Wagner, W. C. Ellis, *Appl. Phys. Lett.* **1964**, *4*, 89–90; b) Y. Wu, P. Yang, *J. Am. Chem. Soc.* **2001**, *123*, 3165–3166; c) Y.-J. Hsu, S.-Y. Lu, *Chem. Commun.* **2004**, 2102–2103; d) Y.-J. Hsu, S.-Y. Lu, Y.-F. Lin, *Adv. Func. Mater.* **2005**, *15*, 1350–1357.

[2] a) T. J. Trentler, K. M. Hickman, S. C. Goel, A. M. Viano, P. C. Gibbons, W. E. Buhro, *Science* **1995**, *270*, 1791–1794; b) J. D. Holmes, K. P. Johnston, R. C. Doty, B. A. Korgel, *Science* **2000**, *287*, 1471–1473; c) H.-Y. Tuan, D. C. Lee, T. Hanrath, B. A. Korgel, *Chem. Mater.* **2005**, *17*, 5705–5711; d) F. Wang, A. Dong, J. Sun, R. Tang, H. Yu, W. E. Buhro, *Inorg. Chem.* **2006**, *45*, 7511–7521.

[3] a) V. F. Puntes, K. M. Krishnan, A. P. Alivisatos, *Science* **2001**, *291*, 2115–2117; b) Z. A. Peng, X. Peng, *J. Am. Chem. Soc.* **2001**, *123*, 1389–1395; c) Z. A. Peng, X. G. Peng, *J. Am. Chem. Soc.* **2002**, *124*, 3343–3353; d) Y. Yin, A. P. Alivisatos, *Nature* **2005**, *437*, 664–670.

[4] a) H. T. Liu, A. P. Alivisatos, *Nano Lett.* **2004**, *4*, 2397–2401; b) D. J. Milliron, S. T. Hughes, Y. Cui, L. Manna, J. Li, L.-W. Wang, A. P. Alivisatos, *Nature* **2004**, *430*, 190–195; c) Y. Cui, U. Banin, M. T. Björk, A. P. Alivisatos, *Nano Lett.* **2005**, *5*, 1519–1523; d) D. Tarì, M. D. Giorgi, F. D. Sala, L. Carbone, R. Krahne, L. Manna, R. Cingolani, *Appl. Phys. Lett.* **2005**, *87*, 224101.

[5] a) L. Manna, D. J. Milliron, A. Meisel, E. C. Scher, A. P. Alivisatos, *Nat. Mater.* **2003**, *2*, 382–385; b) B. Q. Sun, E. Marx, N. C. Greenham, *Nano Lett.* **2003**, *3*, 961–963; c) E. C. Scher, L. Manna, A. P. Alivisatos, *Philos. Trans. R. Soc. London, Ser. A* **2003**, *361*, 241–257; d) I. Gur, N. A. Fromer, A. P. Alivisatos, *J. Phys. Chem. B* **2006**, *110*, 25543–25546.

[6] a) H. Q. Yan, R. He, J. Pham, P. D. Yang, *Adv. Mater.* **2003**, *15*, 402–405; b) Y. Dai, Y. Zhang, Z. L. Wang, *Solid State Commun.* **2003**, *126*, 629–633; c) C. Ronning, N. G. Shang, I. Gerhards, H. Hofsäss, M. Seibt, *J. Appl. Phys.* **2005**, *98*, 034307; d) Y. Ding, Z. L. Wang, T. Sun, J. Qiu, *Appl. Phys. Lett.* **2007**, *90*, 153510.

[7] a) Y. W. Jun, S. M. Lee, N. J. Kang, J. Cheon, *J. Am. Chem. Soc.* **2001**, *123*, 5150–5151; b) M. Chen, Y. Xie, J. Lu, Y. J. Xiong, S. Y. Zhang, Y. T. Qian, X. M. Liu, *J. Mater. Chem.* **2002**, *12*, 748–753; c) K.-T. Yong, Y. Sahoo, M. T. Swihart, P. N. Prasad, *J. Phys. Chem. C* **2007**, *111*, 2447–2458;d) H. Chu, X. Li, G. Chen, W. Zhou, Y. Zhang, Z. Jin, J. Xu, Y. Li, *Cryst. Growth Des.* **2005**, *5*, 1801–1806.

[8] a) L. Manna, E. C. Scher, A. P. Alivisatos, *J. Am. Chem. Soc.* **2000**, *122*, 12700–12706;b) J. W. Grebinski, K. L. Hull, J. Zhang, T. H. Kosel, M. Kuno, *Chem. Mater.* **2004**, *16*, 5260–5272; c) R. Xie, U. Kolb, T. Basché, *Small* **2006**, *2*, 1454–1457; d) K.-T. Yong, Y. Sahoo, M. T. Swihart, P. N. Prasad, *Adv. Mater.* **2006**, *18*, 1978–1982; e) S. Asokan, K. M. Krueger, V. L. Colvin, M. S. Wong, *Small* **2007**, *3*, 1164–1169.

[9] a) S. D. Bunge, K. M. Krueger, T. J. Boyle, M. A. Rodriguez, T. J. Headley, V. L. Colvin, *J. Mater. Chem.* **2003**, *13*, 1705–1709; b) W. W. Yu, Y. A. Wang, X. G. Peng, *Chem. Mater.* **2003**, *15*, 4300–4308; c) L. Carbone, S. Kudera, E. Carlino, W. J. Parak, C. Giannini, R. Cingolani, L. Manna, *J. Am. Chem. Soc.* **2006**, *128*, 748–755; d) J.-Y. Zhang, W. W. Yu, *Appl. Phys. Lett.* **2006**, *89*, 123108.

[10] C.-Y. Yeh, Z. W. Lu, S. Froyen, A. Zunger, *Phys. Rev. B* **1992**, *46*, 10086–10097.

[11] a) Y.-J. Hsu, S.-Y. Lu, *Langmuir* **2004**, *20*, 194–201; b) Y.-J. Hsu, S.-Y. Lu, *Chem. Commun.* **2004**, 2102–2103; c) Y.-J. Hsu, S.-Y. Lu, Y.-F. Lin, *Adv. Func. Mater.* **2005**, *15*, 1350–1357.

[12] a) G. Perna, S. Pagliara, V. Capozzi, M. Ambrico, T. Ligonzo, *Thin Solid Films* **1999**, *349*, 220–224; b) V. B. Patil, G. S. Shahane, D. S. Sutrave, B. T. Raut, L. P. Deshmukh, *Thin Solid Films* **2004**, *446*, 1–5.

[13] a) G. Shen, C.-J. Lee, *Cryst. Growth Des.* **2005**, *5*, 1085–1089; b) Y.-F. Lin, Y.-J. Hsu, S.-Y. Lu, S.-C. Kung, *Chem. Commun.* **2006**, 2391–2393.

[14] a) Y. D. Li, H. W. Liao, Y. Ding, Y. Fan, Y. Zhang, Y. T. Qian, *Inorg. Chem.* **1999**, *38*, 1382–1387; b) J. Yang, J.-H. Zeng, S.-H. Yu, L. Yang, G.-E. Zhou, Y.-T. Qian, *Chem. Mater.* **2000**, *12*, 3259–3263; c) D. Xu, Z. Liu, J. o. Liang, Y. Qian, *J. Phys. Chem. B* **2005**, *109*, 14344–14349.

Received: August 30, 2007
Revised: January 3, 2008

